Front. Earth Sci. 2025, 19(2): 232–245
https://doi.org/10.1007/s11707-024-1112-3

RESEARCH ARTICLE

Spatial associations between electric power consumption in three major urban agglomerations of China via a len of nighttime light index

Wenyi LIU[1], Jie ZHOU[2], Huaqiao XING[1], Peiyuan QIU[1], Yaohui LIU (✉)[1,3]

1 School of Surveying and Geo-Informatics, Shandong Jianzhu University, Jinan 250101, China
2 School of Geography and Tourism, Qilu Normal University, Jinan 250013, China
3 College of Geodesy and Geomatics, Shandong University of Science and Technology, Qingdao 266590, China

Abstract Electricity constitutes a fundamental pillar of both the national economy and contemporary lifestyles. Monitoring electric power consumption (EPC) has important implications for energy planning, energy conservation and emission reduction, energy security, and smart city development. However, the current monitoring and evaluation of EPC is less accurate and does not allow for real-time monitoring and evaluation of EPC. This study established an EPC assessment model based on EPC data, nighttime light remote sensing technology, and GIScience methodology, aiming to analyze the spatiotemporal variation of EPC in three major urban agglomerations of China from 2012 to 2020 and estimate EPC in 2025. Furthermore, the spatial correlation of EPC was explored using Moran' s *I* spatial analysis method. The results indicate that the established model has an average accuracy of 77.56% and can be used for accurate and real-time estimation of EPC. The EPC showed an increasing trend from 2012 to 2020, with the Yangtze River Delta urban agglomeration (YRD) exhibiting the highest growth rate, as high as 49.60%. The EPC in the Beijing-Tianjin-Hebei urban agglomeration (BTH) showed a negative spatial correlation. However, the YRD and the Guangdong-Hong Kong-Macao Greater Bay Area urban agglomeration (GBA) exhibited significant positive spatial correlation in EPC. The findings of this study serve a scientific basis and reference data for the development of energy policies and strategies. Furthermore, this study can help to achieve the "carbon peaking and carbon neutrality goals" proposed by the Chinese government.

Keywords nighttime lights, EPC, dynamic monitoring, spatial analysis, three major urban agglomerations of China

Received September 3, 2023; accepted December 13, 2023

E-mail: liuyaohui20@sdjzu.edu.cn

1 Introduction

As a terminal energy source, the consumption of electricity has been continuously growing, and the structure, scale, and development trend of EPC have a close correlation with economic development and people' s well-being (Buechler et al., 2022; Kahouli et al., 2022). China's EPC has undergone significant and profound variations with the gradual shift toward high-quality economic development and industrial restructuring, coupled with the evolving lifestyle patterns of the populace (Li et al., 2022a; Wang et al., 2022b). However, China's extensive territory and uneven distribution of resources have led to a disconnect between electricity production and consumption, necessitating provinces to engage in mutual power supply adjustment, and to some extent, break the administrative regional barriers (Li et al., 2022b; Liu et al., 2023). Consequently, spatio-temporal dynamic monitoring and variance analysis of EPC assume a pivotal role in ensuring a stable and sustainable electricity supply. Meanwhile, they also contribute to the realization of the "dual-carbon" goal and sustainable human development (Atiku et al., 2022; Guzović et al., 2022).

Several studies have been conducted on power monitoring (Rakhmonov et al., 2022; Satrovic and Adedoyin, 2022). Kivchun (2021) has explored a technique for predicting the EPC of technological objects by utilizing the values of the transformed vector rank distribution. Hamed et al. (2022) have developed econometric models that predict the annual consumption of electricity. Torres et al. (2022) have proposed a novel EPC model known as long short-term memory (LSTM), which exhibits the capacity to process sequential data. While various power consumption monitoring methods are available, a comprehensive analysis shows that the above techniques have certain limitations, on the one

hand, the accuracy of EPC assessment and prediction is low, on the other hand, it is not possible to monitor and assess the EPC in real-time (Shi et al., 2018).

Nighttime light remote sensing is an optical remote sensing technique that can detect shimmering light during the night, providing quick, accurate, and objective information about the ground surface and human activities (Yu et al., 2015; Liang et al., 2020; Chen et al., 2021, 2023; Liu et al., 2023a). Since most of the night's steady light is from the city's man-made light source, the nighttime light remote sensing image is more intuitive to reflect human activity at night (Yang et al., 2019; Adelabu et al., 2022; Wang et al., 2022a; Liu et al., 2023c). As a new monitoring method, nighttime light has the merits of wide coverage, quick timeliness, and easy access, making it suitable for studying urban issues on a multi-scale and long-term basis (Chen et al., 2019; Zheng et al., 2019b; Pan et al., 2020; Liu et al., 2023b). It has been widely applied in disaster monitoring, economic and population development monitoring, and urban expansion monitoring (Li et al., 2018; Fan et al., 2019) and has proven to be a useful tool in monitoring and analyzing EPC at various scales (Xie and Weng, 2016; Li et al., 2019; Lu et al., 2019; Lin and Shi, 2020; Dlamini and Dlamini, 2022). For instance, Ahmad et al. (2022) used nighttime light data to measure the EPC growth from 2000 to 2020. Shi et al. (2016) detected variations in global EPC during the period 1992 to 2013 based on nighttime light data. Cao et al. (2014) used nighttime light data to estimate the spatial distribution of EPC in China and analyzed the spatiotemporal variations of EPC from 1994 to 2009. Zhao et al. (2020) combined nighttime light data with toponym and points-of-interest data to estimate EPC in ethnic minority rural areas at a high spatial resolution. Overall, using nighttime light data for EPC monitoring and analysis is a promising approach that can complement other existing methods.

In the current context of global energy constraints and climate change, EPC monitoring is critical for sustainable development and energy management (Auffhammer, 2022; Olabi and Abdelkareem, 2022). As the economic and population centers of the country, the EPC of China's three major urban agglomerations, including BTH, YRD, and GBA, is of great importance for energy supply and environmental impact (Wang et al., 2022c; Yang et al., 2022). Monitoring EPC in these urban agglomerations can provide valuable data and insights to help assess energy use efficiency, carbon emission levels, and energy demand trends to guide sustainable energy planning and management. Moreover, due to the large size and complexity of these urban agglomerations, monitoring EPC can also help optimize energy supply, improve energy security, and provide fundamental support for smart city development. Therefore, the choice of monitoring EPC in China's three major urban agglomerations is an important step to promoting sustainable development, optimizing energy use as well as achieving smart city goals.

This study aims to construct a fitting model to estimate the EPC of China's three major urban agglomerations timely and accurately. We first utilized national polar-orbiting partnership visible infrared imaging radiometer suite (NPP-VIIRS) nighttime light data and EPC data from 2012 to 2020 to construct the fitting model of the total nighttime light index (TNLI) and EPC. Meanwhile, we investigated the spatiotemporal variation of EPC. Then the 2021 data was used for verification, and EPC for 2025 was estimated. Moreover, Moran's I were conducted to identify the spatial patterns and trends in EPC. The model provided in this study can realize real-time high-precision monitoring and assessment of EPC, which can be used as a decision-making basis for estimating the future trend of China's economy and promoting the rational allocation of power resources.

The rest of this study is organized as follows. Section 2 introduces the study area and data, the processing method of nighttime light data, the fitting model construction, and the spatial correlation analysis method. Section 3 introduces the spatiotemporal variations of EPC in the BTH, YRD, and GBA of China from 2012 to 2020 and the fitting model of TNLI and EPC. The discussion and conclusion are presented in Sections 4 and 5, respectively.

2 Study area and data

2.1 Study area

This study focuses on three major urban agglomerations in China (BTH, YRD, and GBA), which are presented in Fig. 1. The BTH, situated in the heart of the Bohai Sea Rim in North-east Asia, is the largest and most dynamic region in northern China. With a gross domestic product (GDP) of 8.8 trillion yuan as of 2020 and a permanent population of 110 million, this agglomeration represents a significant economic and demographic hub. The YRD is renowned for its highly active economic development, strong innovation capacity, and an impressive degree of openness in China. With a permanent population of 170 million and a GDP of 20.5 trillion yuan as of 2020, this agglomeration is a vital economic and innovation center in China. The GBA, surrounded by mountains on three sides and converged by three rivers, benefits from vast sea areas and good port groups that have contributed to its economic prominence in China. With a GDP of 11.6 trillion yuan as of 2020 and a permanent population of 90 million, this agglomeration is a critical economic hub and a significant contributor to China's economy (He et al., 2019; Yang et al., 2021).

2.2 Data

2.2.1 Nighttime light data

The NPP-VIIRS product has a spatial resolution of

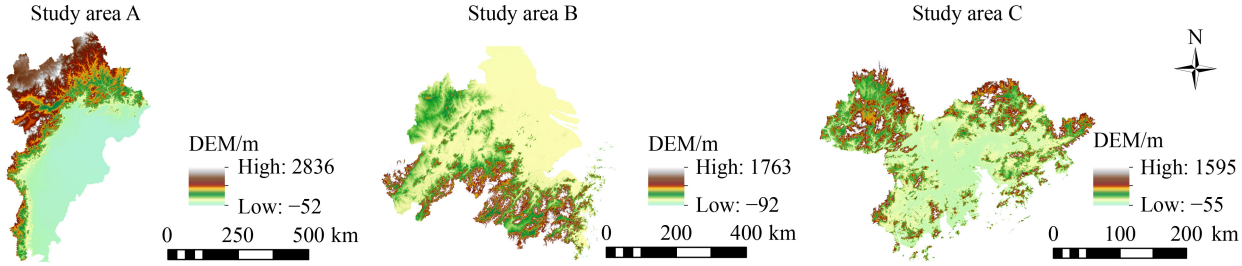

Fig. 1 Study area.

approximately 750 m, which has the advantages of high spatial resolution, global coverage, long-term continuous observation, and strong data consistency and comparability. This data is derived from Earth Observation Group website. It can provide a powerful tool for researchers to analyze and understand the distribution and changes of nighttime lights on the Earth's surface (Yu et al., 2018, 2019). Moreover, it can be used to construct a reliable model for monitoring and evaluating EPC (Zheng et al., 2019a; Liu et al., 2022). Furthermore, the NPP-VIIRS nighttime light data have been subjected to radiation correction, resulting in an improvement in data quality. This study selected monthly nighttime light data from January to December (excluding May to July) from 2012 to 2021.

2.2.2 EPC data

The EPC data for each city in the study area are primarily obtained from the Statistical Yearbooks of various provinces and cities from 2012 to 2021.

3 Methodology

3.1 Nighttime light data processing and calculation

To ensure accurate calculation and comparison of the nighttime light index, it is essential to address negative or abnormal values in the NPP-VIIRS data. This requires a series of preprocessing steps, such as removing negative values, image cutting, projection transformation, and resampling the nighttime light data (Chen et al., 2021; Liu et al., 2023). Additionally, to enable effective comparison and analysis of data from different days while eliminating noise, normalization of the nighttime light data is necessary.

Due to the effect of stray light pollution, there is a severe distortion in the light data of middle and high regions of China in summer (all cell values are 0), which is concentrated in the data from May to July, therefore the light data from May to July is excluded when using monthly data to synthesize annual data, and the other 9 months of light data from 2012 to 2021 are used to generate annual light data. The *TNLI* is selected for calculation and analysis:

$$TNLI_m = \sum_{i=1}^{n} DN_i, \tag{1}$$

$$TNLI = \frac{\sum_{i=1}^{4} TNLI_m + \sum_{i=8}^{12} TNLI_m}{9}, \tag{2}$$

where $TNLI_m$ is the total nighttime light index for each monthly data, n is the number of rasters, DN_i is the cell radiation value corresponding to each raster cell.

3.2 Construction of the fitting model

Based on the significant linear correlation between *TNLI* and *EPC*, we establish a power consumption estimation model, and its calculation equation is

$$EPC = aTNLI + b, \tag{3}$$

where *EPC* is the estimated *EPC*, *TNLI* is the total nighttime light index, and a and b are the regression coefficients.

3.3 Normalization of EPC

To explore the spatial variations trend of *EPC*, the *EPC* in the three study areas from 2012 to 2021 was normalized. The normalization is calculated by Eq. (4).

$$M_i = \frac{N_i - N_{\min}}{N_{\max} - N_{\min}}, \tag{4}$$

where M_i is the normalized value, N_i is the statistical data, $N_{\max}$ is the maximum statistics, and $N_{\min}$ is the minimum statistic.

3.4 Moran's *I* statistics model

This study employs Global Moran's *I* and local indicators of spatial association (LISA) to examine the spatiotemporal dynamics of *EPC*. Global Moran's *I* is determined using Eq. (5), yielding values ranging from −1 to 1 (Moran, 1948). Values closer to 1 indicate a stronger positive correlation, while values closer to −1 indicate a stronger negative correlation. Values close to 0 indicate a lack of significant correlation. Local Moran's *I*, calculated using Eq. (6), further analyses the correlation of spatial units. LISA analysis utilizes five attributes to

describe the correlation among these units, including "High-High", "Low-Low", "High-Low", "Low-High", and "Not Significant":

$$I = \frac{\sum_{i=1}^{n}\sum_{j=1}^{n}\omega_{ij}(x_i-\bar{x})(x_j-\bar{x})}{\frac{1}{n}\sum_{i=1}^{n}(x_i-\bar{x})^2\cdot\sum_{i=1}^{n}\sum_{j=1}^{n}\omega_{ij}}, \quad (5)$$

$$I_i = \frac{x_i-\bar{x}}{\frac{1}{n}\sum_{i=1}^{n}(x_i-\bar{x})^2}\sum_{j=1,j\neq i}^{n}\omega_{ij}(x_j-\bar{x}), \quad (6)$$

where n is the number of regions, x_i is the EPC of the ith region, $\bar{x}$ is the mean value, and w_{ij} is the spatial symmetric weight.

4 Results

4.1 Temporal Variations of EPC

The trends of EPC in the study area from 2012 to 2020 are presented in Fig. 2. During this period, showing an increasing trend. Among the three urban agglomerations, the YRD had the highest EPC and the fastest growth rate, increasing by 49.60%. The BTH exhibited a moderate EPC level, but its growth rate is relatively lower, with an increase of 24.29%. The GBA recorded the lowest EPC levels, but it demonstrated a relatively fast growth rate, with a 42.25% increase. However, in 2020, all three urban agglomerations experienced a decrease in their growth rates, which could be attributed to the impact of the corona virus disease 2019 (COVID-19) pandemic. The pandemic had widespread effects on various sectors of society, resulting in the suspension of many industrial enterprises, reduced activity levels among residents, and home isolation measures. These factors collectively contributed to a slowdown in the growth of EPC during that particular year.

The EPC of BTH is presented in Fig. 3. The results indicate an overall increasing trend in the EPC of all cities in the region from 2012 to 2020. Among the cities, Beijing, Tianjin, and Tangshan exhibited high and rapid EPC, with an average annual EPC of more than 80 billion kWh, accounting for 28.69%, 24.31%, and 22.80% of the total annual EPC of the BTH, respectively. Notably, in 2016, the EPC of Beijing surpassed 100 billion kWh. Conversely, Hengshui, Zhangjiakou, Qinhuangdao, and Chengde exhibited lower EPC levels and slower growth rates, with an average annual EPC of less than 20 billion kWh. Hengshui had the lowest EPC in the region, while Beijing had the highest. Specifically, Beijing's average annual EPC was 7.25 times that of Hengshui.

The EPC of the YRD is presented in Fig. 4. The results indicate an overall increasing trend in the EPC of all cities in the region from 2012 to 2020. Notably, Shanghai and Suzhou exhibited high and rapid EPC, with an average annual EPC of more than 130 billion kWh, accounting for 42.03% and 39.77% of the total annual EPC of the YRD, respectively. The EPC of Shanghai and Suzhou exceeded 150 billion kWh in 2017. However, Zhoushan, Chizhou, Tongling, and Anqing reported lower EPC and slower growth, with an average annual EPC of less than 10 billion kWh. Zhoushan had the lowest EPC in the region, while Shanghai had the highest. Specifically, Shanghai's average annual EPC was 26.43 times that of Zhoushan.

The EPC of the GBA is presented in Fig. 5. The results indicate an overall increasing trend in the EPC of all cities in the region from 2012 to 2020. Notably, Shenzhen and Guangzhou demonstrated high and rapid EPC growth, with an average annual EPC of over 80 billion kWh, accounting for 22.01% and 21.96% of the total annual EPC of the GBA, respectively. The EPC of Shenzhen and Guangzhou exceeded 90 billion kWh in 2018. Conversely, Macao exhibited the lowest EPC and the slowest growth, with an average annual EPC of just over 5 billion kWh. Shenzhen had the highest EPC, while Macao had the lowest. Specifically, Shenzhen's average annual EPC was 16.47 times that of Macao.

4.2 Spatial variations of EPC

The EPC from 2012 to 2020 within the three study areas

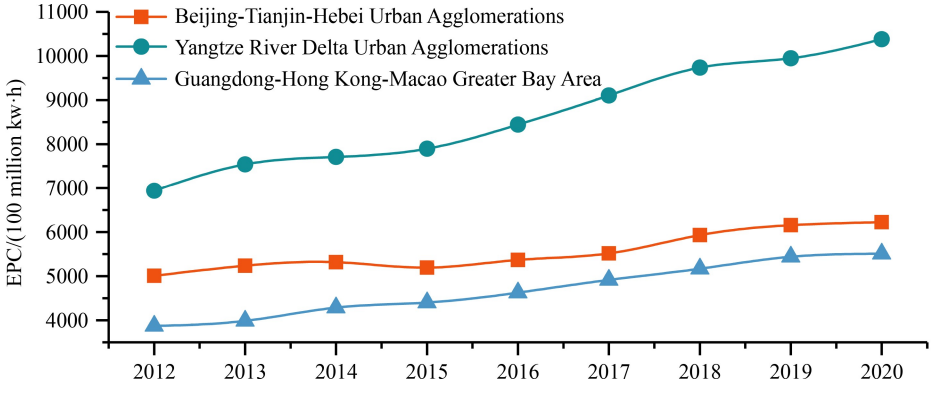

Fig. 2 Temporal variations of EPC in the three major urban agglomerations from 2012 to 2020.

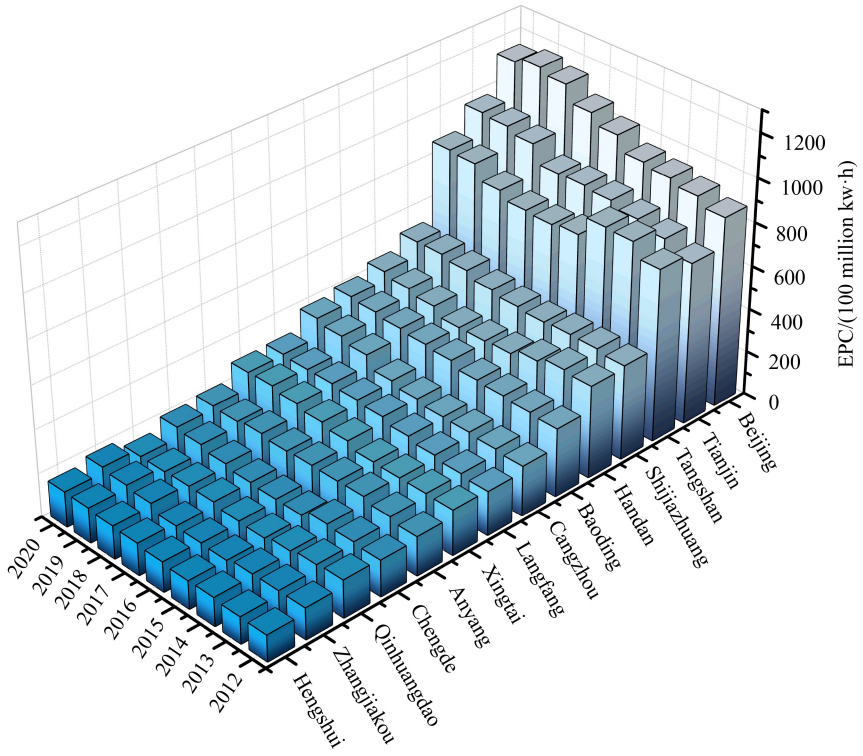

Fig. 3 Temporal variations of EPC in the BTH from 2012 to 2020.

was normalized, followed by division into five average-grade intervals ranging from 0 to 1. The spatial variations of EPC in the BTH are presented in Fig. 6. The overall distribution is relatively high in the Beijing-Tianjin-Tangshan compared to the northern and southern regions, with the southern region exhibiting a more rapid growth rate than the northern region. Specifically, in 2016, Beijing exhibited a significant surge in EPC, surpassing a

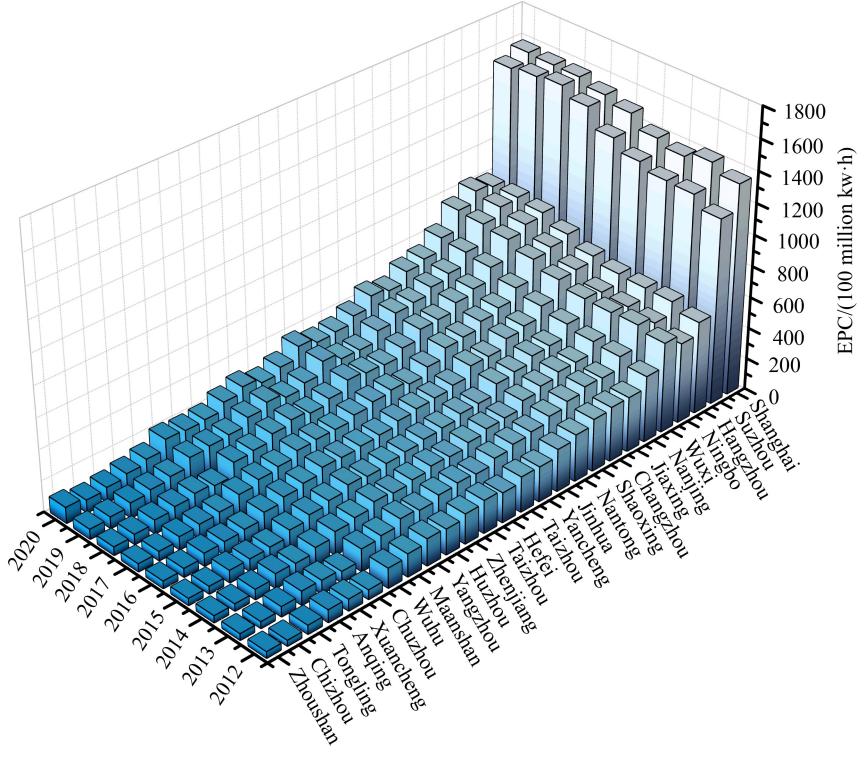

Fig. 4 Temporal variations of EPC in the YRD from 2012 to 2020.

normalized value of 0.8. Similarly, in 2019, Tianjin demonstrated a remarkable increase in EPC, with a normalized value exceeding 0.8. Conversely, Tangshan's EPC exhibited relative stability, ranging between 0.6 to 0.8 in terms of normalized values.

The spatial variations of EPC of the YRD are presented in Fig. 7, revealing high values in the eastern and southern areas, and lower values in the western and northern areas. Notably, Shanghai and Suzhou emerge as the cities with the highest EPC levels, consistently surpassing a normalized value of 0.8, with Shanghai maintaining this high level consistently. Furthermore, in 2015 Suzhou experienced a significant surge in EPC, exceeding a normalized value of 0.8. Similarly, Hangzhou witnessed a substantial increase in EPC in 2016, with a normalized value surpassing 0.4. Additionally, in 2017 both Wuxi and Ningbo observed noteworthy increments in EPC, surpassing a normalized value of 0.4.

The spatial variations of EPC of the GBA are presented in Fig. 8, with high values in the middle and eastern areas and low in the west. Notably, among the cities encompassed within the GBA, Shenzhen, Guangzhou, and Dongguan stand out for exhibiting the highest EPC values. Specifically, in 2016, both Shenzhen and Guangzhou witnessed a substantial increase in EPC, surpassing a normalized value of 0.8. In 2019, Dongguan's EPC normalized value exceeded 0.8, while Foshan's EPC normalized value surpassed 0.6 in 2017. Additionally, significant EPC improvements were observed in Jiangmen and Huizhou, with Huizhou's normalized EPC value exceeding 0.6 in 2020.

4.3 Fitting model

The nighttime light data from 2012 to 2021 underwent processing, with the data from 2012 to 2020 selected for constructing the fitting model, while the data from 2021 were utilized to verify the accuracy of the model. Figures 9−11 depict the nighttime light maps at intervals every five years. The findings reveal a consistent upward trend in nighttime light intensity, exhibiting a pronounced correlation with the spatial distribution of EPC. Notably, cities such as Beijing, Tianjin, Tangshan, Shanghai, Suzhou, Shenzhen, and Guangzhou, located within the BTH, YRD, and GBA regions, exhibit a significant increase in lighting intensity over the examined period.

The fitting models, as shown in Figs. 12−14, demonstrate a robust correlation between TNLI and EPC within the three study areas. Specifically, the BTH presented a correlation coefficient R^2 of 0.7593, while the YRD had an R^2 of 0.8764, and the GBA had an R^2 of 0.8554. Thus, the YRD returned the highest degree of correlation between TNLI and EPC, followed by the GBA, while the BTH displayed a relatively lower level of correlation.

4.4 Validation of fitting model

Based on the above fitting model, *TNLI* and EPC in 2021 were selected for accuracy verification in each region, focusing on the estimation of estimated EPC by

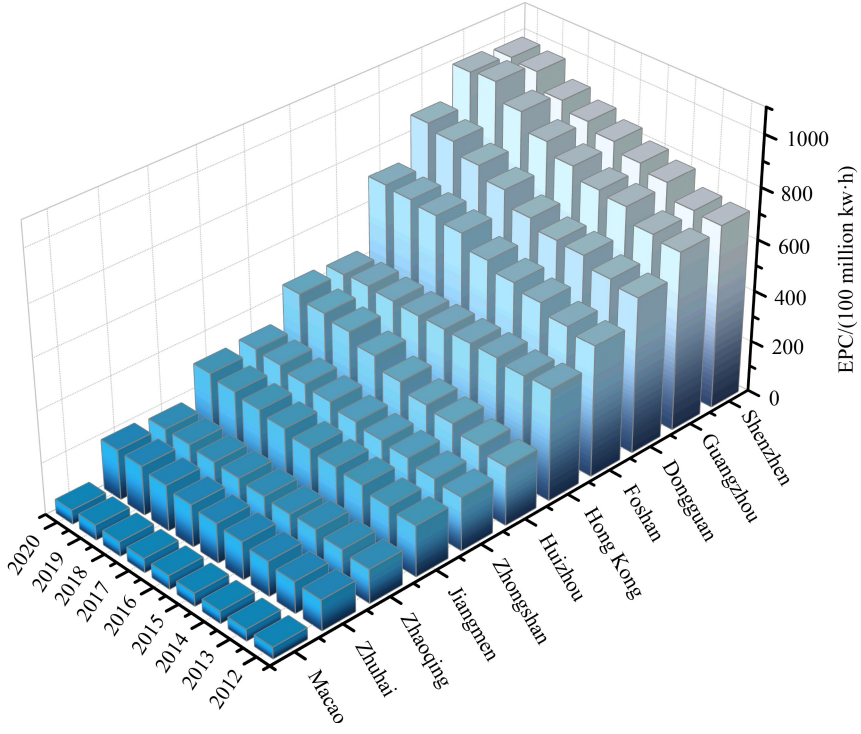

Fig. 5 Temporal variations of EPC in the GBA from 2012 to 2020.

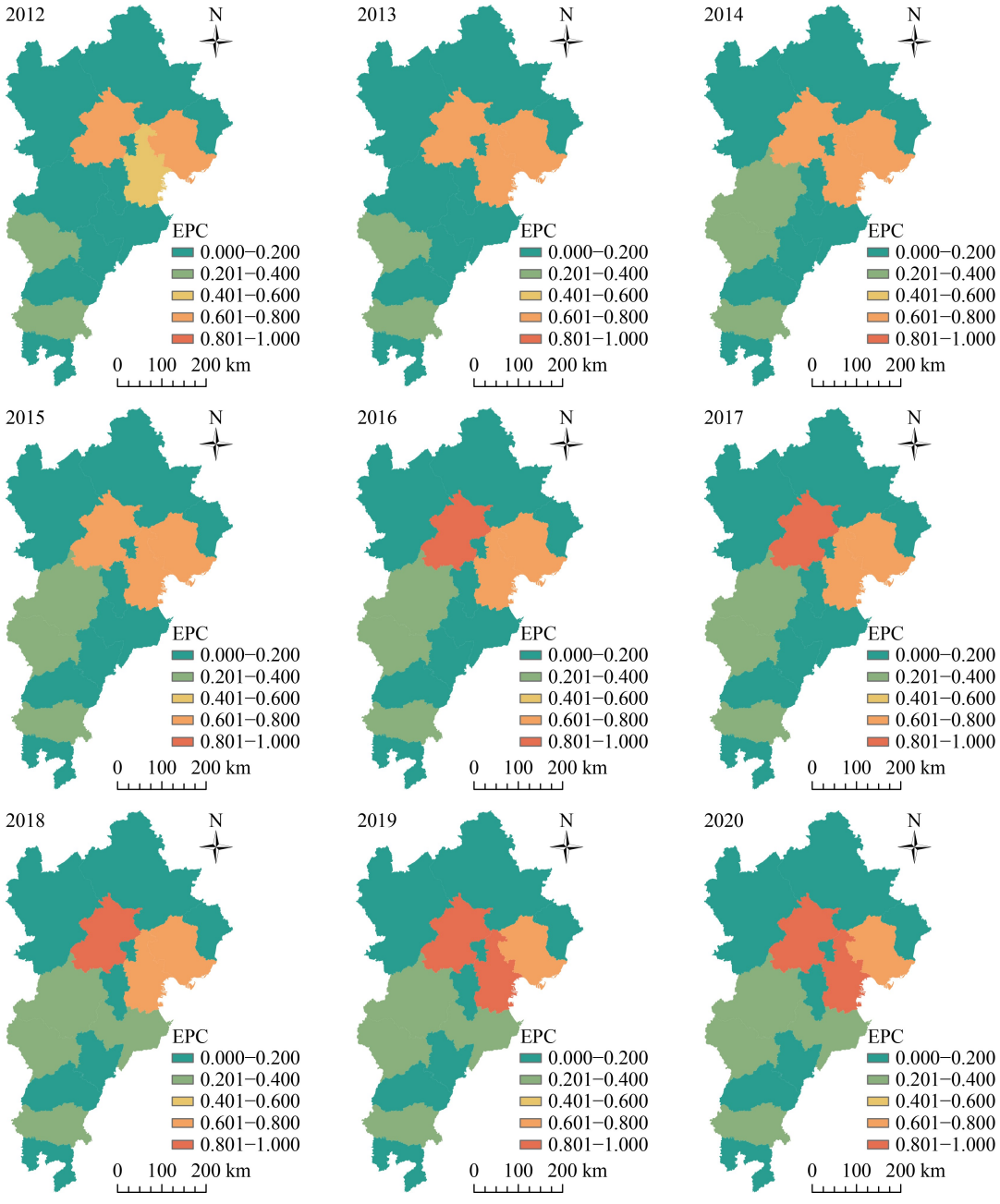

Fig. 6 Spatial variations of EPC in the study area A from 2012 to 2020.

incorporating *TNLI* into the corresponding urban agglomeration's fitting model. This estimation was then compared with the actual EPC, allowing for the computation of the associated error. Subsequently, the average estimation accuracy of each region within the study area was calculated, representing the overall estimation accuracy. The verification results are presented in Table 1. Notably, the YRD exhibited the highest average estimation accuracy of 79.84%, closely followed by the GBA with 79.04%. However, the BTH displayed a relatively lower average estimation accuracy of 73.81%. Furthermore, the fitting model estimated an increase in EPC, suggesting that by 2025, the total EPC for the BTH, YRD, and GBA regions would reach 720 billion kWh, 1.4 trillion kWh, and 680 billion kWh, respectively. These findings emphasize the potential of nighttime light as a reliable foundation for achieving accurate and real-time estimation of EPC.

4.5 Global spatial correlation analysis

This study aimed to conduct a global spatial correlation analysis of the EPC. The calculated results are presented in Table 2, where *p*-values represent the rejection domain probability. The findings reveal that the changes of Moran's *I* of EPC of BTH are relatively apparent, all of

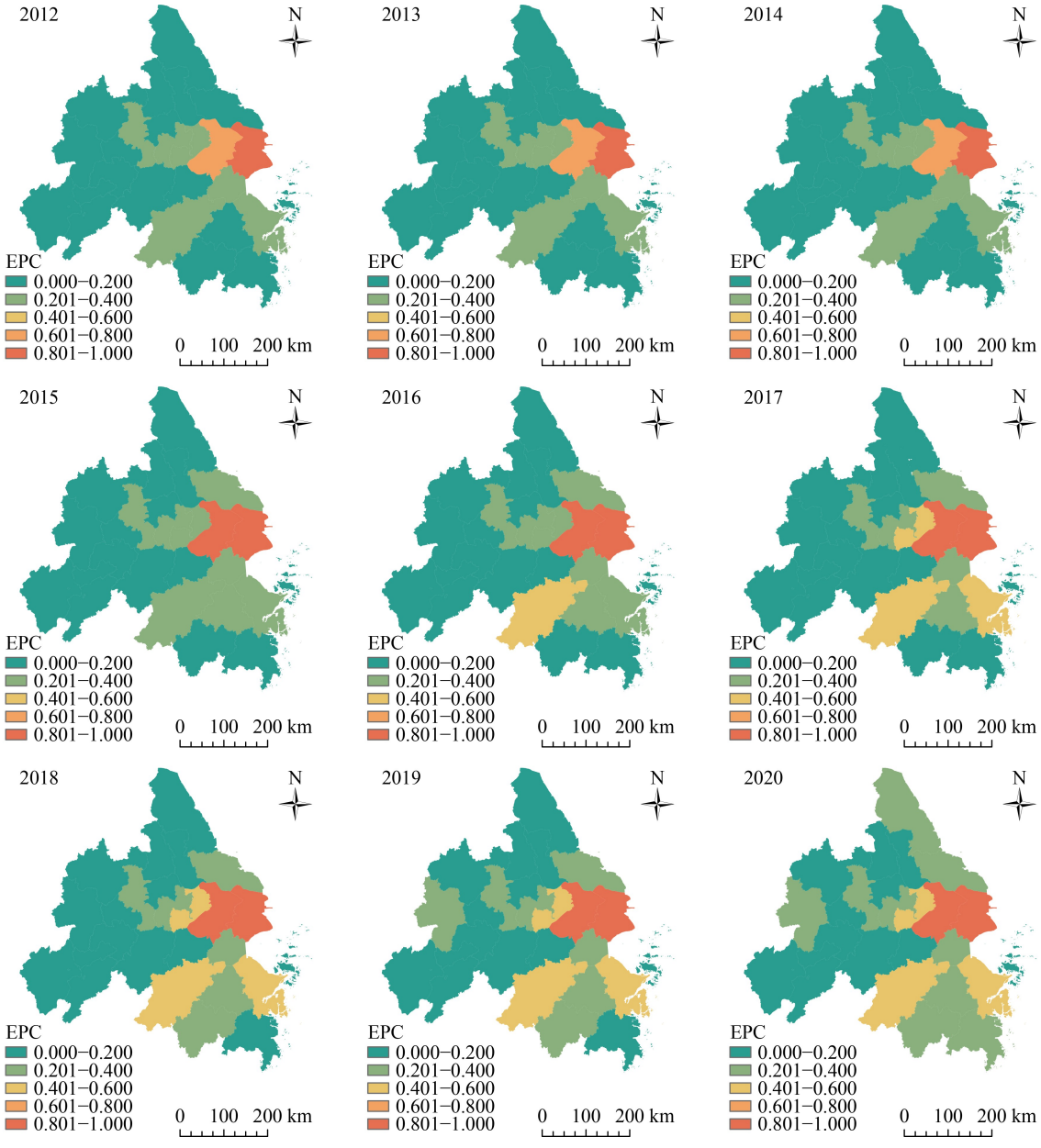

Fig. 7 Spatial variations of EPC in the study area B from 2012 to 2020.

them are less than 0, and the *p*-values are also less than 0.1, indicating that EPC passes the significance test at a 90% confidence level and presents a negative spatial correlation. On the other hand, the spatial agglomeration type of EPC in YRD is relatively stable, with Moran's *I* greater than 0 and *p*-values less than 0.01, indicating that EPC passes the significance test at a 99% confidence level and presents a positive spatial correlation. Similarly, the spatial agglomeration types of EPC in the GBA are also relatively stable, with Moran's *I* greater than 0 and *p*-values less than 0.05, indicating that EPC passes the significance test at a 95% confidence level and presents a positive spatial correlation. These different spatial agglomeration patterns of EPC in the three urban agglomerations highlight the need for targeted policies to effectively manage and reduce energy consumption in these regions.

4.6 Local spatial correlation

The local spatial correlation analysis of EPC is presented in Fig. 15. The local spatial correlation of EPC in the BTH from 2012 to 2020 remained consistent, with a low-high type of spatial pattern dominating. This pattern was predominantly observed in the northern part of the agglomeration, including Langfang, Chengde, and Zhangjiakou, which are contiguous to the high EPC region of the BTT. Thus, a Low-High spatial correlation pattern was evident. Figure 16 demonstrated that the local spatial correlation of EPC in the YRD from 2012 to 2020

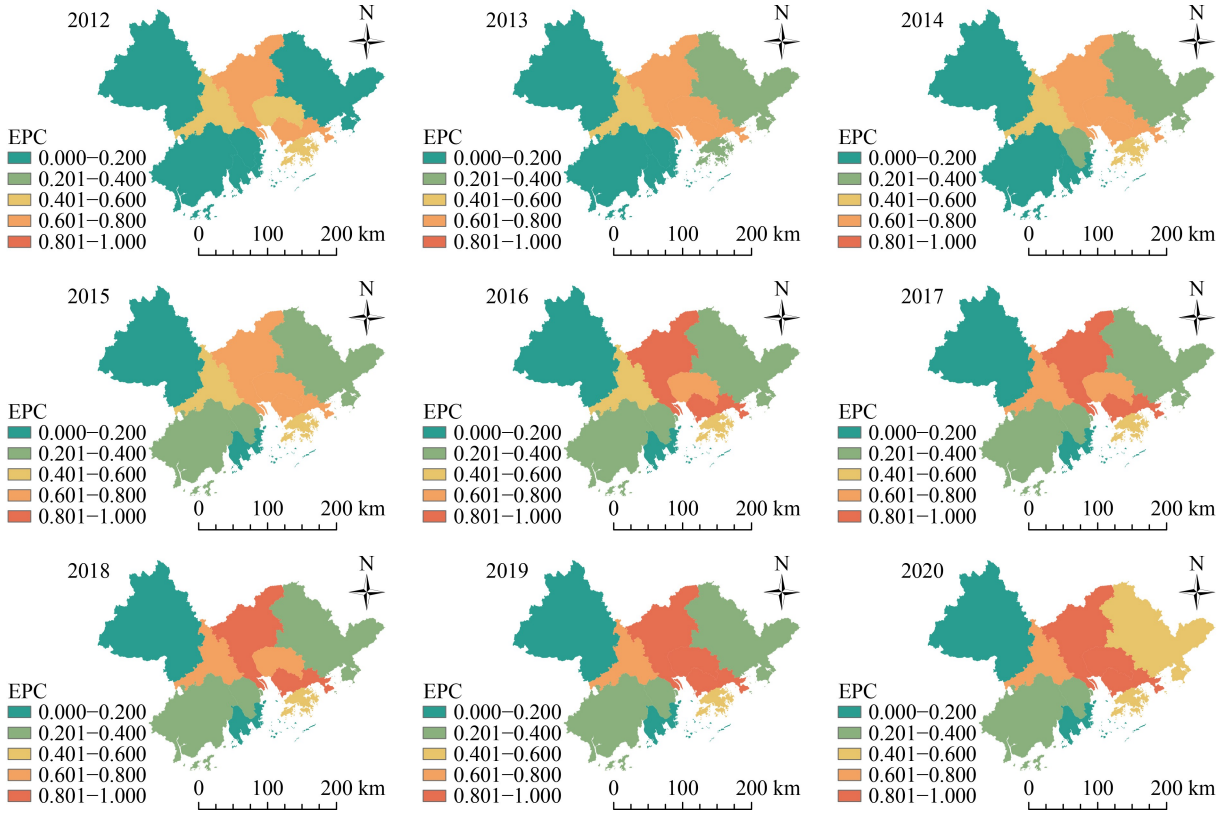

Fig. 8 Spatial variations of EPC in the study area C from 2012 to 2020.

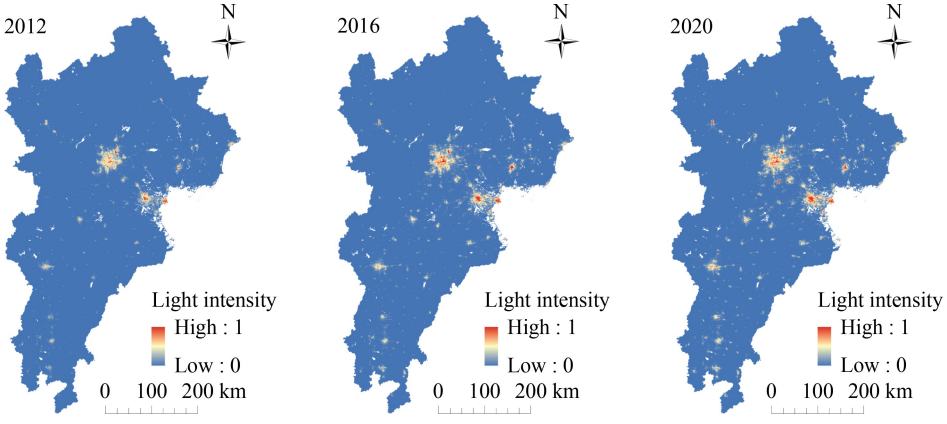

Fig. 9 Nighttime light variations in the study area A from 2012 to 2020.

also remained constant, with significant spatial patterns primarily demonstrating High-High and Low-Low types. The High-High type is mainly distributed in the eastern part of the agglomeration, including Shanghai, Suzhou, and Jiaxing, exemplifying the convergence effect of high EPC with neighboring areas. Therefore, the High-High type was prevalent. The Low-Low type was mostly observed in the western part of the agglomeration, including Anqing, Chizhou, Tongling, and Hefei, indicating the convergence effect of low EPC with neighboring regions, and thereby demonstrating a Low-Low spatial correlation pattern. Moreover, Figure 17 indicated that the local spatial correlation of EPC in the GBA experienced significant changes from 2012 to 2020. During this period, the spatial pattern primarily showed Low-Low and Low-High types from 2012 to 2016. The Low-Low type was mainly concentrated in the southern part of the agglomeration, including Zhuhai and Macao, signifying the convergence effect of low EPC with neighboring regions and thus presenting a Low-Low spatial correlation pattern. The Low-High type was mainly concentrated in the eastern part of the agglomeration, with Huizhou being the main city, adjacent to areas with high EPC such as Shenzhen and Guangzhou. Consequently, the Low-High spatial correlation pattern was evident. In 2016, Dongguan

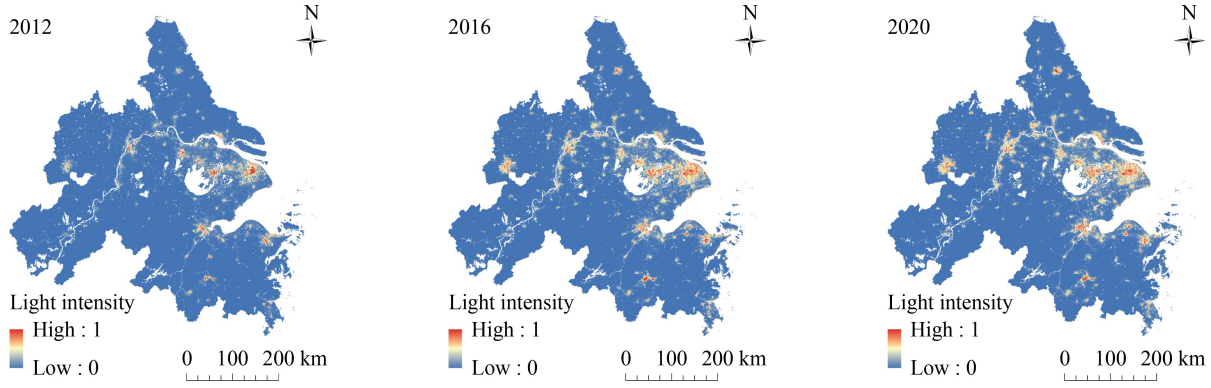

Fig. 10 Nighttime light variations in the study arae B from 2012 to 2020.

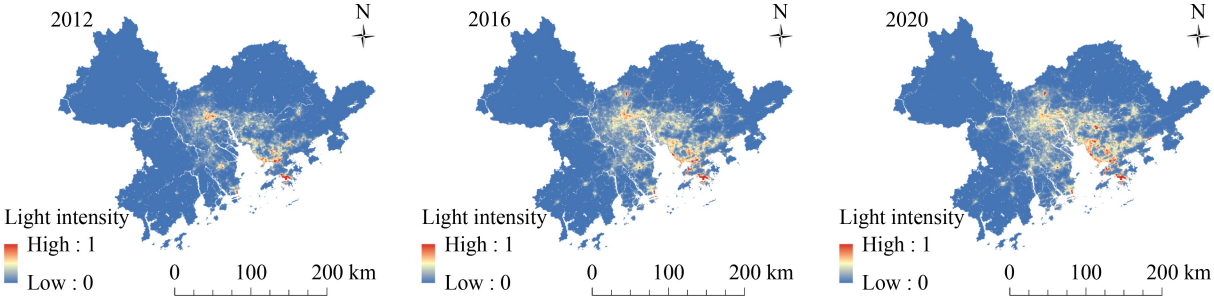

Fig. 11 Nighttime light variations in the study area C from 2012 to 2020.

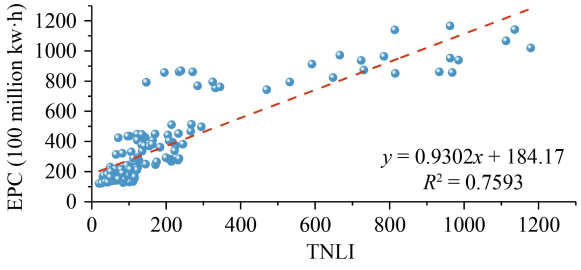

Fig. 12 *TNLI* and EPC fitting model of the BTH.

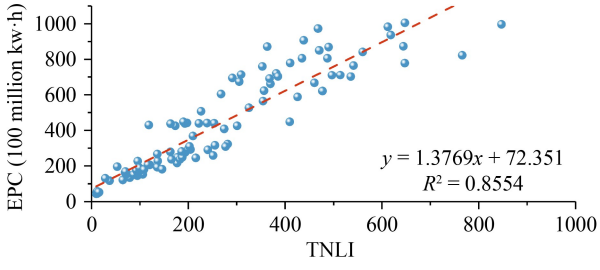

Fig. 14 *TNLI* and EPC fitting model of the GBA.

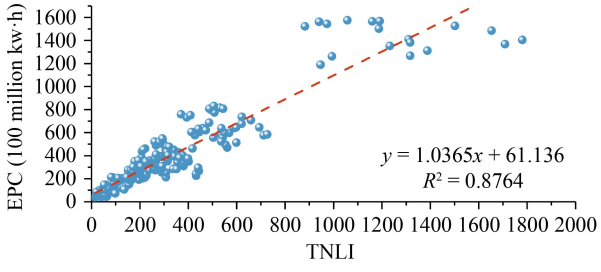

Fig. 13 *TNLI* and EPC fitting model of the YRD.

Table 1 The accuracy of the fitting model for the three major urban agglomerations

Region	Average estimate accuracy
BTH	73.81%
YRD	79.84%
GBA	79.04%

Table 2 Global spatial correlation of EPC in the three urban agglomerations

Region	BTH		YRD		GBA	
Year	Moran's *I*	*P*	Moran's *I*	*P*	Moran's *I*	*P*
2012	−0.092	0.939	0.323	0.003	0.255	0.033
2016	−0.038	0.835	0.324	0.003	0.249	0.035
2020	−0.051	0.889	0.326	0.004	0.255	0.032

transitioned from a No-Significant type to a High-High type, indicating a significant increase in EPC for Dongguan in that year, demonstrating the convergence effect of high EPC with neighboring Shenzhen and Guangzhou. In 2020, the Low-High type in Huizhou disappeared, suggesting an increase in Huizhou's EPC driven by neighboring areas, while Zhuhai and Macao continued to exhibit the Low-Low type, demonstrating the convergence effect of low EPC. In summary, from 2012 to 2020, the growth trend of EPC in the BTH and the YRD exhibited a relatively synchronized pattern, with

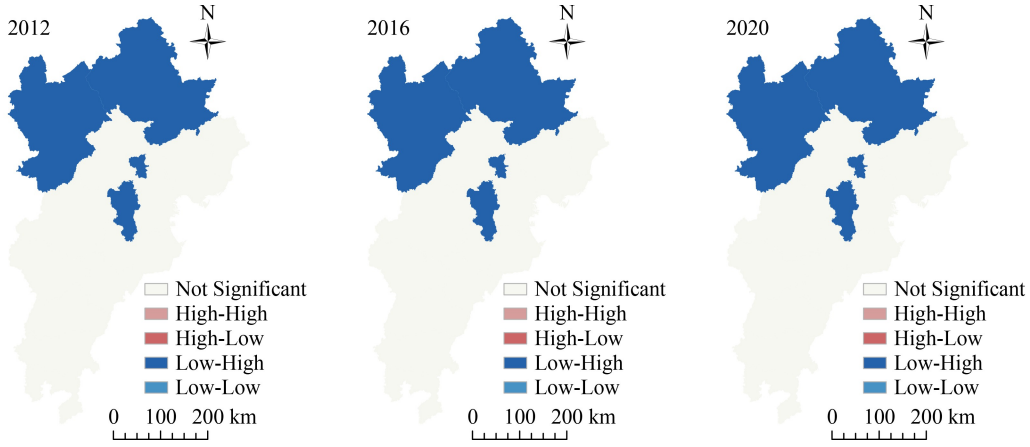

Fig. 15 Local spatial correlation of EPC in the study area A from 2012 to 2020.

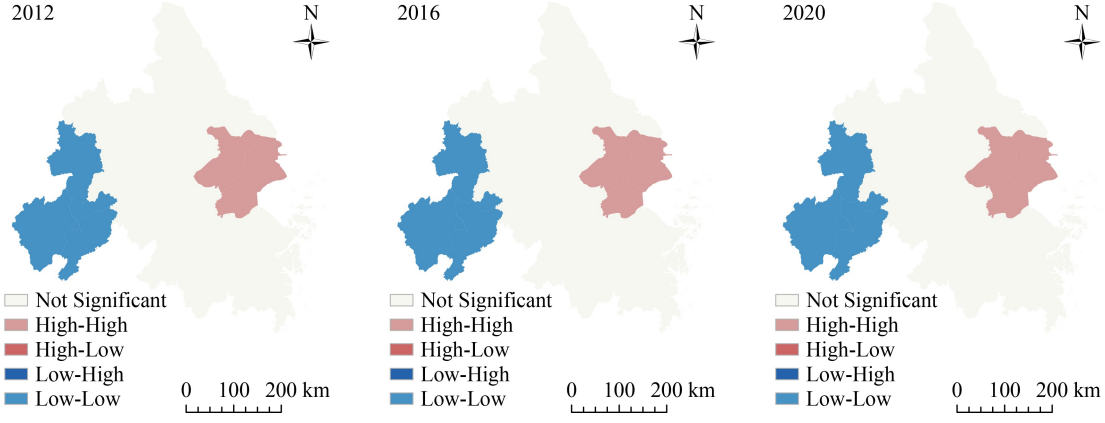

Fig. 16 Local spatial correlation of EPC in the study area B from 2012 to 2020.

local spatial correlation patterns remaining unchanged. In contrast, the growth trend of EPC in certain regions of the GBA displayed notable distinctions, resulting in a significant change in local spatial correlation.

5 Discussion

The spatial distribution of EPC is closely related to nighttime light intensity. In this study, we constructed an EPC monitoring and assessment model based on nighttime light data and EPC data. Furthermore, we comprehensively analyzed the spatial and temporal trends of EPC in China's three major urban agglomerations from 2012 to 2020. The EPC in the three urban agglomerations shows an overall upward trend from 2012 to 2020. This growth is driven by various factors such as economic development, population growth and urbanization. Spatial correlation analyses using Moran's *I* show very different patterns in the three urban agglomerations. In BTH, EPC returns a negative spatial correlation, indicating that high and low EPC areas are clustered together. By contrast, the EPC shows positive spatial correlations in the YRD and GBA, indicating a convergence effect, with areas with high EPC clustering together.

The higher EPC in Beijing can be attributed to it being the capital city of China and an important political, economic, and cultural center. It hosts numerous industries, businesses, government offices, and a large population, leading to higher energy demands. Tianjin is a major port city and an industrial hub, contributing to its moderate growth rate. Tangshan, with stable growth, might have a more balanced industrial and residential consumption mix. Shanghai and Suzhou are major economic and financial centers, hosting numerous multinational corporations and industries. Their higher EPC levels can be attributed to their strong economic activities and larger populations. The lower EPC levels in cities like Zhoushan, Chizhou, Tongling, and Anqing might be due to their comparatively smaller size and less industrial development. Shenzhen and Guangzhou are major technology and industrial centers, contributing to their higher EPC levels. Shenzhen, in particular, is known for its thriving tech industry and rapid economic development. Macao, on the other hand, relies heavily on tourism and gaming, which might explain its lower EPC and slower growth rate. Overall, the differences in EPC among the three urban agglomerations can be attributed to factors such as the level of industrialization, economic activities, population size, and the presence of major

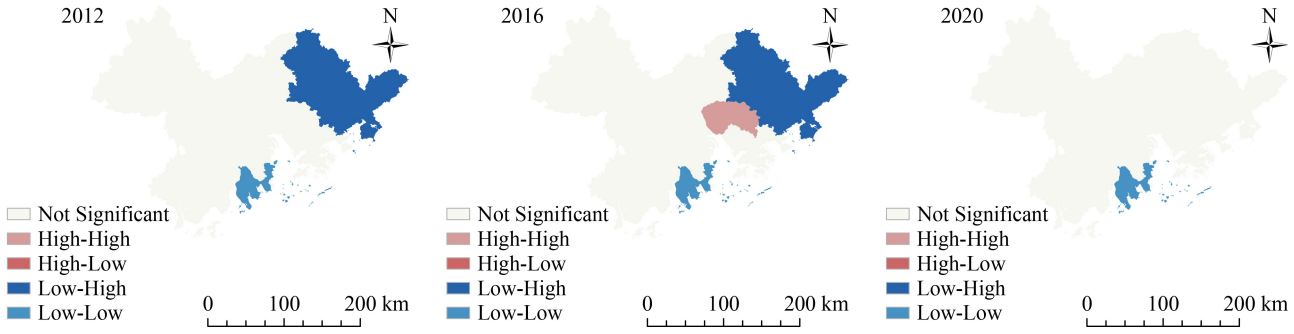

Fig. 17 Local spatial correlation of EPC in the study area C from 2012 to 2020.

commercial and financial centers. Additionally, government policies and investments in infrastructure, energy efficiency measures, and the availability of renewable energy sources may also influence EPC variations across the regions.

To improve the power distribution system in China, a comprehensive approach to encompassing multiple facets is essential. Two crucial strategies are needed to improve the electricity distribution system and promote the utilization of clean energy.

1) Improve the power distribution system. A key priority is addressing the disparities in EPC across the three major urban agglomerations and within different regions within these agglomerations. This necessitates a coordinated effort to strategically plan and deploy renewable energy sources and conventional power generation, while simultaneously strengthening the interconnections between national and local power planning entities. Furthermore, market price signals should be taken into consideration during the planning and construction phases of power systems to ensure economic viability and efficiency.

2) Promote the use of clean energy. While traditional fossil fuels such as coal continue to play a crucial role in ensuring energy security and power system reliability, they also pose significant environmental risks. As China's EPC continues to rise annually, it is imperative to increase the share of renewable energy sources such as wind, solar, and hydropower in the overall power generation mix. Prioritizing the integration of clean energy into the power supply infrastructure will lead to an increased proportion of clean energy in the overall energy mix, thereby reducing the environmental impact associated with power generation.

While this study provides valuable insights into EPC trends and spatial patterns, further research is needed to understand the underlying drivers of EPC in different cities. Factors such as industrial structure, electricity policy and lifestyle choices may influence EPC patterns and should be explored in more detail. Moreover, this study is only based on nighttime light data for model construction, in the future study, we will use the other remote sensing data and statistical data to further improve the accuracy of EPC monitoring and assessment. Meanwhile, it is also possible to evaluate EPC based on daily nighttime light data to realize daily monitoring of EPC.

In conclusion, the analysis of EPC trends and spatial patterns in the three urban agglomerations provides policy makers and researchers with valuable information that can help rationalize the allocation of electricity in the three urban agglomerations. Also contribute to the development of targeted strategies for sustainable energy management and urban development in China. The findings can guide balancing economic growth with environmental sustainability and electricity efficiency.

6 Conclusions

This study established an EPC assessment model based on EPC and NPP-VIIRS nighttime light data to investigate the spatiotemporal changes in EPC within the three major urban agglomerations in China from 2012 to 2020. Furthermore, EPC for 2025 in the study areas was estimated based on this model. Finally, global and local spatial correlation were performed to identify the spatial patterns and trends in EPC. The main conclusions drawn from this study are as following.

1) The fitting model of *TNLI* and EPC in each region demonstrates high accuracy with an average estimation accuracy of 77.56%.

2) An overall increase in EPC from 2012 to 2020, with the highest growth rate observed in the YRD. At the municipal scale, a negative spatial correlation of EPC was observed. The dominant spatial pattern is characterized by a Low-High type.

3) In the YRD, Shanghai and Suzhou have higher EPC and faster growth rates. The EPC exhibits a significant spatial positive correlation at the municipal scale, indicating a clustering and distribution trend. The local spatial pattern is manifested through High-High and Low-Low types.

4) In the GBA, Shenzhen and Guangzhou have higher EPC and faster growth rates. The EPC exhibits a significant spatial positive correlation at the municipal scale. The local spatial correlation changes significantly, with the significant spatial types primarily being Low-

Low and Low-High from 2012 to 2016.

As remote sensing technology continues to advance, future power consumption simulation and estimation using nighttime light data will increasingly rely on multi-source data with higher accuracy and timeliness. To this end, a simulation model will be developed to establish a dynamic monitoring system between daily, monthly, quarterly, and annual satellite remote sensing data and EPC at various scales in China. This will provide a scientific basis for decision-making and enable a more rational allocation of power resources, thereby facilitating informed projections of China's future economic trends.

Acknowledgement This work was supported by the National Natural Science Foundation of China (Grant No. 42201077); the Natural Science Foundation of Shandong Province (No. ZR2021QD074); the China Postdoctoral Science Foundation (No. 2023M732105); the Youth Innovation Team Project of Higher School in Shandong Province, China (No. 2024KJH087).

Data Availability Statement The data sets generated during and/or analyzed during the current study are available from the corresponding author on reasonable request.

Competing interests The authors declare that they have no competing interests.

References

Adelabu S, Mncube Z, Adagbasa E (2022). Utilising VIIRS DNB nighttime light data together with landsat daytime data to assess changes in light pollution in Ethekwini Metropolitan Municipality (EMM). Int Arch Photogramm Remote Sens Spat Inf Sci, 43: 463–470

Ahmad M N, Cheng Q, Luo F (2022). Dynamic linkage between urbanization, electrical power consumption, and suitability analysis using remote sensing and GIS techniques. Photogramm Eng Remote Sensing, 88(3): 171–179

Atiku A M, Ismail S, Roslan F, Ahmad A U (2022). The effect of electricity distribution loos, electricity power consumption, electricity intensity on energy consumption in West Africa. Int J Energy Econ Polic, 12(5): 361–369

Auffhammer M (2022). Climate adaptive response estimation: short and long run impacts of climate change on residential electricity and natural gas consumption. J Environ Econ Manage, 114: 102669

Buechler E, Powell S, Sun T, Astier N, Zanocco C, Bolorinos J, Flora J, Boudet H, Rajagopal R (2022). Global changes in electricity consumption during COVID-19. iScience, 25(1): 103568

Cao X, Wang J, Chen J, Shi F (2014). Spatialization of electricity consumption of China using saturation-corrected DMSP-OLS data. Int J Appl Earth Obs Geoinf, 28: 193–200

Chen Z, Yu B, Ta N, Shi K, Yang C, Wang C, Zhao X, Deng S, Wu J (2019). Delineating seasonal relationships between Suomi NPP-VIIRS nighttime light and human activity across Shanghai, China. IEEE J Sel Top Appl Earth Obs Remote Sens, 12(11): 4275–4283

Chen Z, Yu B, Yang C, Zhou Y, Yao S, Qian X, Wang C, Wu B, Wu J (2021). An extended time series (2000–2018) of global NPP-VIIRS-like nighttime light data from a cross-sensor calibration. Earth Syst Sci Data, 13(3): 889–906

Chen Z, Yu S, You X, Yang C, Wang C, Lin J, Wu W, Yu B (2023). New nighttime light landscape metrics for analyzing urban-rural differentiation in economic development at township: a case study of Fujian province, China. Appl Geogr, 150: 102841

Dlamini W M, Dlamini L C (2022). Spatial assessment and monitoring of household electricity access and use using nighttime lights and ancillary spatial data: a case of Eswatini. Afr Geograph Rev, 41(3): 299–317

Fan X, Nie G, Deng Y, An J, Zhou J, Li H (2019). Rapid detection of earthquake damage areas using VIIRS nearly constant contrast night-time light data. Int J Remote Sens, 40(5−6): 2386–2409

Guzović Z, Duic N, Piacentino A, Markovska N, Mathiesen B V, Lund H (2022). Recent advances in methods, policies and technologies at sustainable energy systems development. Energy, 245: 123276

Hamed M M, Ali H, Abdelal Q (2022). Forecasting annual electric power consumption using a random parameters model with heterogeneity in means and variances. Energy, 255: 124510

He Q, Zeng C, Xie P, Tan S, Wu J (2019). Comparison of urban growth patterns and changes between three urban agglomerations in China and three metropolises in the USA from 1995 to 2015. Sustain Cities Soc, 50: 101649

Kahouli B, Nafla A, Trimeche H, Kahouli O (2022). Understanding how information and communication technologies enhance electric power consumption and break environmental damage to reach sustainable development. Energy Build, 255: 111662

Kivchun O (2021). Forecasting electric power consumption of technocenosis objects on the basis of values from transformed vector rank distribution. J Phys: Conference Series, Volume 1901, V International Scientific and Technical Conference "Mechanical Science and Technology Update" (MSTU 2021), 16-17 March 2021, Omsk, Russia

Li J, Ho M S, Xie C, Stern N (2022a). China's flexibility challenge in achieving carbon neutrality by 2060. Renew Sustain Energy Rev, 158: 112112

Li Q, Yang L, Jiang F, Liu Y, Guo C, Han S (2022b). Distribution characteristics, regional differences and spatial convergence of the water-energy-land-food nexus: a case study of China. Land (Basel), 11(9): 1543

Li S, Cheng L, Liu X, Mao J, Wu J, Li M (2019). City type-oriented modeling electric power consumption in China using NPP-VIIRS nighttime stable light data. Energy, 189: 116040

Li X, Zhan C, Tao J, Li L (2018). Long-term monitoring of the impacts of disaster on human activity using DMSP/OLS nighttime light data: a case study of the 2008 Wenchuan, China Earthquake. Remote Sens (Basel), 10(4): 588

Liang H, Guo Z, Wu J, Chen Z (2020). GDP spatialization in Ningbo City based on NPP/VIIRS night-time light and auxiliary data using random forest regression. Adv Space Res, 65(1): 481–493

Lin J, Shi W (2020). Statistical correlation between monthly electric power consumption and VIIRS nighttime light. ISPRS Int J Geoinf, 9(1): 32

Liu H, Yang C, Chen Z (2023). Differentiated improvement path of carbon emission efficiency of China's provincial construction

industry: a fuzzy-set qualitative comparative analysis approach. Buildings, 13(2): 543

Liu L, Li Z, Fu X, Liu X, Li Z, Zheng W (2022). Impact of power on uneven development: evaluating built-up area changes in Chengdu based on NPP-VIIRS images (2015–2019). Land (Basel), 11(4): 489

Liu Y, Liu W, Lin Y, Zhang X, Zhou J, Wei B, Nie G, Gross L (2023a). Urban waterlogging resilience assessment and postdisaster recovery monitoring using NPP-VIIRS nighttime light data: a case study of the 'July 20, 2021'heavy rainstorm in Zhengzhou City, China. Int J Disaster Risk Reduct, 90: 103649

Liu Y, Liu W, Qiu P, Zhou J, Pang L (2023b). Spatiotemporal evolution and correlation analysis of carbon emissions in the nine provinces along the Yellow River since the 21st century using nighttime light data. Land (Basel), 12(7): 1469

Liu Y, Liu W, Zhang X, Lin Y, Zheng G, Zhao Z, Cheng H, Gross L, Li X, Wei B, Su F (2023c). Nighttime light perspective in urban resilience assessment and spatiotemporal impact of COVID-19 from January to June 2022 in mainland China. Urban Clim, 50: 101591

Lu L, Weng Q, Xie Y, Guo H, Li Q (2019). An assessment of global electric power consumption using the defense meteorological satellite program-operational linescan system nighttime light imagery. Energy, 189: 116351

Moran P (1948). The interpretation of statistical maps. J R Stat Soc Series B Stat Methodol, 10(2): 243–251

Olabi A, Abdelkareem M A (2022). Renewable energy and climate change. Renew Sustain Energy Rev, 158: 112111

Pan W, Fu H, Zheng P (2020). Regional poverty and inequality in the Xiamen-Zhangzhou-Quanzhou city cluster in China based on NPP/VIIRS night-time light imagery. Sustainability (Basel), 12(6): 2547

Rakhmonov I, Najimova A, Esemuratova S M, Koptileuov T (2022). Development of a method for determining the main and additional factors affecting the forecast of electricity consumption. AIP Conf Proc: 070024

Satrovic E, Adedoyin F F (2022). An empirical assessment of electricity consumption and environmental degradation in the presence of economic complexities. Environ Sci Pollut Res Int, 29(52): 78330–78344

Shi K, Chen Y, Yu B, Xu T, Yang C, Li L, Huang C, Chen Z, Liu R, Wu J (2016). Detecting spatiotemporal dynamics of global electric power consumption using DMSP-OLS nighttime stable light data. Appl Energy, 184: 450–463

Shi K, Yu B, Huang C, Wu J, Sun X (2018). Exploring spatiotemporal patterns of electric power consumption in countries along the Belt and Road. Energy, 150: 847–859

Torres J, Martínez-Álvarez F, Troncoso A (2022). A deep LSTM network for the Spanish electricity consumption forecasting. Neural Comput Appl, 34(13): 10533–10545

Wang G, Peng W, Xiang J, Ning L, Yu Y (2022a). Modelling spatiotemporal carbon dioxide emission at the urban scale based on DMSP-OLS and NPP-VIIRS data: a case study in China. Urban Clim, 46: 101326

Wang X, Yan G, Mu X, Xie D, Xu J, Zhang Z, Zhang D (2022b). Human activity changes during COVID‐19 lockdown in China—a view from Nighttime Light. GeoHealth, 6(8): e2021GH000555

Wang Y, Yin S, Fang X, Chen W (2022c). Interaction of economic agglomeration, energy conservation and emission reduction: evidence from three major urban agglomerations in China. Energy, 241: 122519

Xie Y, Weng Q (2016). World energy consumption pattern as revealed by DMSP-OLS nighttime light imagery. GIsci Remote Sens, 53(2): 265–282

Yang C, Xia R, Li Q, Liu H, Shi T, Wu G (2021). Comparing hillside urbanizations of Beijing-Tianjin-Hebei, Yangtze River Delta and Guangdong–Hong Kong–Macau greater Bay area urban agglomerations in China. Int J Appl Earth Obs Geoinf, 102: 102460

Yang C, Yu B, Chen Z, Song W, Zhou Y, Li X, Wu J (2019). A spatial-socioeconomic urban development status curve from NPP-VIIRS nighttime light data. Remote Sens (Basel), 11(20): 2398

Yang T, Zhou K, Zhang C (2022). Spatiotemporal patterns and influencing factors of green development efficiency in China's urban agglomerations. Sustain Cities Soc, 85: 104069

Yu B, Lian T, Huang Y, Yao S, Ye X, Chen Z, Yang C, Wu J (2019). Integration of nighttime light remote sensing images and taxi GPS tracking data for population surface enhancement. Int J Geogr Inf Sci, 33(4): 687–706

Yu B, Shi K, Hu Y, Huang C, Chen Z, Wu J (2015). Poverty evaluation using NPP-VIIRS nighttime light composite data at the county level in China. IEEE J Sel Top Appl Earth Obs Remote Sens, 8(3): 1217–1229

Yu B, Tang M, Wu Q, Yang C, Deng S, Shi K, Peng C, Wu J, Chen Z (2018). Urban built-up area extraction from log-transformed NPP-VIIRS nighttime light composite data. IEEE Geosci Remote Sens Lett, 15(8): 1279–1283

Zhao F, Ding J, Zhang S, Luan G, Song L, Peng Z, Du Q, Xie Z (2020). Estimating rural electric power consumption using NPP-VIIRS night-time light, toponym and POI data in ethnic minority areas of China. Remote Sens (Basel), 12(17): 2836

Zheng Q, Weng Q, Wang K (2019a). Developing a new cross-sensor calibration model for DMSP-OLS and Suomi-NPP VIIRS night-light imageries. ISPRS J Photogramm Remote Sens, 153: 36–47

Zheng Y, Shao G, Tang L, He Y, Wang X, Wang Y, Wang H (2019b). Rapid assessment of a typhoon disaster based on NPP-VIIRS DNB daily data: the case of an urban agglomeration along Western Taiwan Straits, China. Remote Sens (Basel), 11(14): 1709